JOURNAL OF OPTOELECTRONICS AND ADVANCED MATERIALS, Vol. 11, No. 4, April 2009, p. 380 - 385

Fiber optic method for measuring the intensity of IR radiation

I. P. CULEAC*, Iu. H. NISTOR, M. S. IOVU
Institute of Applied Physics of the Academy of Sciences of Moldova,
Str. Academiei 5, Chisinau MD 2028, Republic of Moldova

A high sensitivity fiber-optic method for registration of infrared (IR) radiation is proposed. The method is based on the effect of modal interference in an optical fiber. The speckle pattern is registered in the far field of a multimode fiber and is processed by a PC for deriving the output signal. The method also can be applied for registration of temperature, mechanical vibrations, etc.

(Received April 13, 2009; accepted April 23, 2009)

Keywords: Optical fiber, Infrared, Modal interference, Speckle pattern

1. Introduction

Existing methods for registration of IR radiation can be basically divided into the following groups: bolometric methods, pyroelectric, photovoltaic, photoconductive methods, as well as mix methods. In the case of bolometer method, the radiation that is absorbed on the surface of the detector changes the temperature. The change in the temperature adducts to raise a change in electrical resistance of sensing element, which easily can be measured by conventional devices. In the case of pyrometers, the change in the temperature induces a change in the electrical dipole moment of the crystal structure, which gives rise to a measurable charge outside the crystal through capacitive coupling. The photodetectors exhibit a higher response speed since the photogenerated charges are swept by the electric field and rapidly gathered up by the outside electrodes. In the case of bolometer or pyroelectric detectors the heat capacity can essentially reduce the registration speed. The photoresistors display a high optical gain, defined as the ratio between the current under lighted conditions and current under dark conditions, but the photoresistors has extremely low speed, since the photogenerated carriers disappear after secession of the radiation only by the effect of recombination.

In this paper, we propose a new fiber optic method for registration of IR radiation, which is based on the effect of constructive and destructive interference of propagating modes in the far field of a multimode optical fiber. The resulting interference image, alternatively the speckle pattern, can be used for registration of the amplitude of infrared radiation that hits the sensing element of the fiber.

2. Experimental results

The experimental set-up is represented in Fig. 1. It consists of a multimode optical fiber, a coherent light source, a microobjective, a CCD detector, and a PC for speckle image processing. Alternatively, the output radiation can be projected on the CCD plane through a pin hole. The probing light from the coherent light source is injected into the input end face of the fiber and at the output end face of the fiber the far-field distribution of the probing light intensity (the speckle pattern) is registered. When a physical perturbation hits the fiber, the speckle pattern is changed. The CCD is used for registration of the variations of the speckle pattern of the multimode fiber.

The probing light source is a He-Ne Laser (λ=633 nm) with the output power of P=10 mW. A multimode optical fiber with a parabolic refractive index profile and the core diameter of about 50 µm was used as a sensing element. As a source of IR radiation, we used a common electrical heater placed opposite the fiber. Variation of the IR radiation intensity was performed by variation of the distance between the optical fiber and the electrical heater. The speckle pattern was registered with a HDCS-1020 CMOS image sensor with the pixel size 7.4x7.4 µm, and image array sizes VGA 640x480. The full frame video rate at 8 bit resolution was 30 fps. A typical speckle pattern of the fiber used for measurements is shown in Fig. 2.

Analyses of the intensity distribution $I(x,y)$ of the probing light in the far-field of the fiber provides information about the conditions of light propagation in the multimode fiber as well as on the perturbations that affect the optical fiber. The speckle image represents the result of destructive and constructive interference of propagating modes in the far field of the fiber (Fig. 3). For a separate mode at the output end of fiber the magnitude of electric field $\vec{E}$ can be represented as:

$$\vec{E} = \vec{E}_0 \cos(\omega t + \varphi), \qquad (1)$$

where $\vec{E}_0$ - is the amplitude of electrical field, φ - the phase of probing light wave $\varphi = 2\pi n_{eff} \dfrac{L}{\lambda}$, L - is the geometrical path length of the *k-th* mode in the fiber, λ – the wavelength of probing light; n_{eff} – the effective refractive index of the fiber, ω – the frequency of electromagnetic wave, and t - is the time.

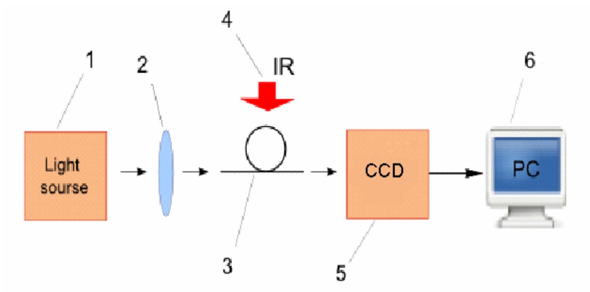

Fig. 1. Schematic representation of the method: 1 – a coherent light source; 2 – microobjective; 3 - the optical fiber, 4 – IR radiation source; 5 - CCD detector; 6 – PC.

The total amplitude of the electric field in any point of speckle pattern in the plane of CCD sensor can be represented as the sum of all contributions of N propagating modes of the fiber:

$$E = \sum_{k=1}^{N} |A_k| \exp(j\varphi_k), \qquad (2)$$

where A_k – is the amplitude of the *k-th* mode of the fiber, φ_k - is the phase for the *k-th* mode at the output end of the fiber, N – is the total number of modes propagating in the core of the fiber.

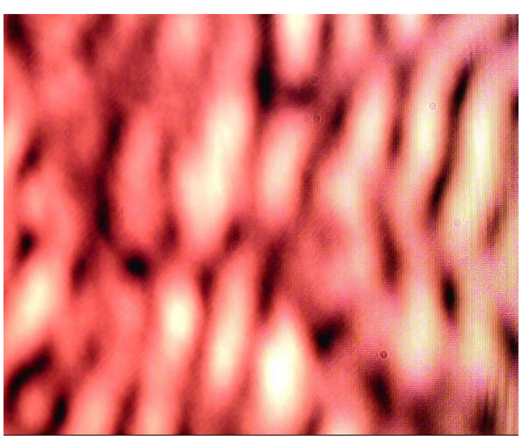

Fig. 2. Illustration of the far field speckle pattern of the fiber.

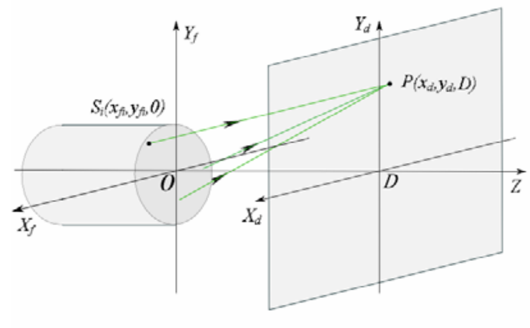

Fig. 3. Schematic representation of interference of the modes in the far field of the fiber

When two modes interfere in the point *P(x,y)* of the CCD plane the resulting intensity *I(x,y)* can be described by the relation:

$$I(x,y) = I_k(x,y) + I_{k+1}(x,y) + 2\sqrt{I_k I_{k+1}} \cos(\varphi_k - \varphi_{k+1}) \qquad (3)$$

where $I_k(x,y)$ and $I_{k+1}(x,y)$ are the intensities of the *k-th* and *(k+1)-th* modes in the point *P(x,y)* of the CCD plane X_dY_d, φ_k and φ_{k+1} are respectively the phase of the *k-th* and *(k+1)-th* modes at the output end of the fiber. The structure of the speckle pattern depends on the coherence properties of the laser beam, refractive index profile, characteristics of the fiber and the external conditions at the core/cladding boundary.

Different modes propagate in an optical fiber with different phase velocities and different modes exhibit different phase shift. The phase shift for the *k-th* mode at the output end of the fiber $\Delta\varphi_k$ can be represented by the relation:

$$\Delta\varphi_k = b_k \Delta L_k + L_k \Delta b_k, \qquad (4)$$

where ΔL_k denotes the change of the geometric path length of the *k-th* mode in the fiber and Δb_k is the change of propagation constant for the *k-th* mode under the action of external perturbation. The phase shift varies under variation of the geometrical path length as well as under variation of the index of refraction. As far as for common multimode fibers the difference of the effective refractive index is much smaller than the effective refractive index $\Delta n_{eff} \langle\langle n_{eff}$, the phase difference $\Delta\varphi$ increases slowly with the increasing of the mode number. The variation of the modes characteristics $\Delta\varphi_k$, ΔL, Δb depends on the refractive index of the optical fiber, refractive index profile, etc. For example, by appropriate selection of the core/cladding material and geometry, refractive index profile and their temperature characteristics and one can dramatically increase the sensitivity of the fiber vs. external perturbations.

The algorithm for processing of the speckle images registered by the CCD camera is based on comparison of original speckle image taken in the initial time moment $t = 0$ and each of the subsequent speckle images, taken in the subsequent time moment t_i. A schematic illustration of the speckle processing algorithm is represented in the Fig. 4. The CCD camera takes an image of the speckle in the initial time t_0, and this image is stored in the buffer memory. The following speckle images are taken in the time t of the consecutive time range t_0 - t_m. Each of the current image I_{in} is subtracted pixel-by-pixel from the initial image I_0 as is described by the relation:

$$I_{in}^{diff} = \left| I_{in}(x,y) - I_{i0}(x,y) \right|, \qquad (5)$$

where I_{in}^{diff} represents the absolute value of the difference of two images' signal taken at the moment i for the n-th pixel with the coordinates (x,y). The next processing step represents summation of all M pixels' signal for determination of the absolute value Sn for the corresponding moment t_i:

$$S_n = \sum_{i=1}^{r1} \sum_{j=1}^{r2} I_n^{diff}(x_i, y_j), \qquad (6)$$

where r_1 and r_2 are the number of pixels along X and Y coordinates respectively. The resulting value of the sum S_{in} is plotted on the PC screen as an output signal of the CCD detector in the time moment t_i (Fig. 5).

Application of this algorithm provides the possibility to plot on the screen in the real-time scale the *difference* of the speckles images. The magnitude S correlate to the amplitude of the perturbation that hits the fiber and can be calibrated to represent exactly the amplitude of the perturbation that affects the fiber. Because we do not utilize too many routines for image processing the rate of the procedure is sufficient high.

On the other hand, because we do not take into account the coordinate of the pixels, this algorithm does not permit to eliminate the elements that are symmetric in the speckle images. Consequently, this reduces the sensitivity and dynamic range of the method. The dependence of the output signal vs. the amplitude of the perturbation keeps linear for a sufficient wide segment of the speckle spot. The output signal that is plotted on the PC screen keeps linear for a sufficient range of IR perturbation (Fig. 6).

3. Computer simulation

As the first step for reducing of the noise was computer simulation of the speckle image and of the corresponding output signal. Experimental results have been compared with computer simulation results.

We have developed a computer simulation of the speckle image in the far-field of the fiber. Consider interference of the modes in the far-field of the fiber. According to the Huygens' principle each of the point in the fiber end face $S(x_f,y_f)$ can be considered as a source of spherical waves (Fig. 3). These waves (modes) interfere constructively or destructively at the output end of the fiber in the image plane of the CCD camera. The speckle pattern represents the contributions of two speckle patterns with a certain mutual phase difference. When external perturbation (heat, IR radiation, et.) hits the fiber the phase difference between these two modes will change.

For a displacement Δd the speckle image is formed at the image plane (CCD target). At each time sequence t_0 and t_i the CCD camera registers a new speckle pattern. The difference of the two speckle images is calculated by subtraction pixel-by-pixel of two images and the value of the sum S_n is calculated with subsequent plotting on the PC monitor.

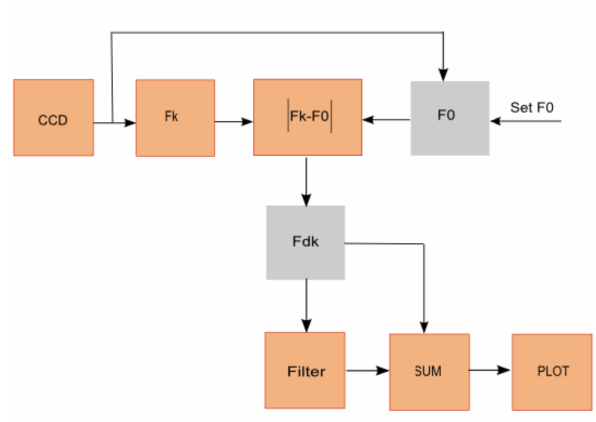

Fig. 4. Illustration of the speckle image processing algorithm

The program for computer simulation of the modal interference in the far-field speckle pattern of the fiber has been developed on the basis of C^{++} language and run on the platform of *Linux*. The PC technical profile is characterized by *AMD Sempron Processor 3000+ 1.61GHz, 1GB RAM*. The basic parameters that have been accepted for numerical simulation have been as follows: CCD resolution, the pixel area S_p, the distance between the end face of the fiber and CCD plane D, the diameter of the core of the fiber d_{core}, the total number of propagating modes N, the wavelength of the probing light λ. Computer simulation of the output signal variation vs. the time after switching on the perturbation IR radiation has been developed.

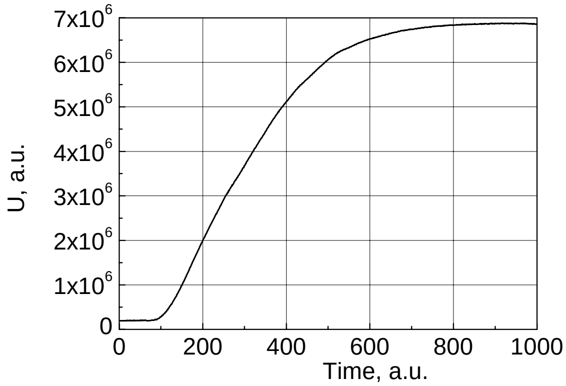

Fig. 5. Signal characteristic after switching on the IR radiation P = 27 µW. The light source is a HeNe laser at 633 nm.

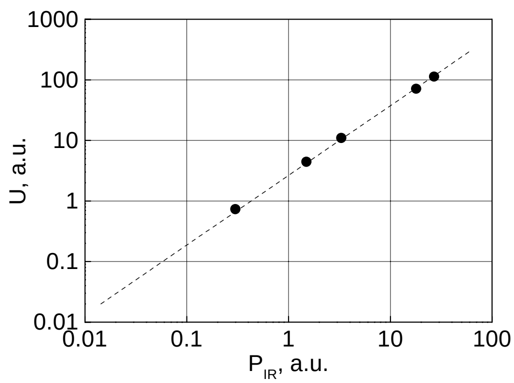

Fig. 6. The amplitude of the output signal vs. the intensity of infrared radiation. The light source is a HeNe laser at 633 nm.

PC simulation has been carried out for two cases: *a)* the ideal case without any noise; *b)* the case when the far-field speckle pattern is composed of "true" signal speckle pattern, accompanied by a speckle noise.

For modeling of the speckle pattern in the far-field of the fiber several points have been chosen randomly on the end face of the fiber. The speckle pattern in the far-field was obtained by coherently adding up the spherical waves originating from the random points. As few as 14 randomly selected points are enough to produce a simulated speckle pattern that correlate quite well with the signal speckle. The distance between the CCD plane and the end face of the fiber was set at 3 cm. The characteristics of the CCD set for simulation have been set of the same values as ones for the real CCD in the experiment (512 x 512 pixels). The result for simulated speckle pattern is represented in Fig. 8. The coordinates of the sources s_i have been generated arbitrarily to follow the relation:

$$x_{fi}^2 + y_{fi}^2 \le \rho^2, \quad i = 1,2,3,\dots N_m, \tag{7}$$

where ρ represents the diameter of the core of the optical fiber. The intensity in the point with the coordinates (x_d, z_d, y_d), that lay in the plane of the CCD sensor ($X_d Y_d$), is determined by the interference of the light waves (modes) generated by the all the source with the coordinate s_i ($x_{fi}, y_{fi}, 0$).

$$I(x_d, y_d) = \frac{\varepsilon_0 c}{T} \int_0^T E^2(x_d, y_d, t)\,dt, \tag{8}$$

where $T = \dfrac{c}{\lambda}$,

$$E(x_d, y_d, t) = \sum_{i=1}^{N_{modes}} E_i(x_d, y_d, t) = \sum_{i=1}^{N_{modes}} E_{0i} \cos\left(2\pi \frac{d_i}{\lambda} - 2\pi \frac{t}{T} + 2\pi \frac{\varphi_i}{\lambda}\right), \tag{9}$$

and $d_i = \sqrt{(x_d - x_{fi})^2 + (y_d - y_{fi})^2 + D^2}$.

d_i is the distance between the source point $s_i(x_f, y_f, 0)$ and the element of the CCD matrix with the coordinates $P(x_d, z_d, D)$.

As far as the index of refraction, n varies very slowly across the fiber cross-section and the optical pathway varies differently for different modes we assumed that the phase of the mode φ_i linearly changes for a small variation of the parameter τ according to the relation:

$$\varphi_i(\tau) = \varphi_{0i} + \delta_i \cdot \tau, \tag{10}$$

where φ_{0i} has been generated arbitrarily for the domain $[0, \lambda]$. The linearity coefficient δ_i has been also generated arbitrarily, so that the phase variation $\Delta\varphi_i$ for each mode is different. The final intensity of the speckle image that contains a noise component is represented as follows:

$$I(x_d, y_d)_{noise} = I(x_d, y_d) + n(x_d, y_d) \tag{11}$$

where $n(x_d, y_d)$ represents the noise, and $I(x_d, y_d)$ represents the true signal.

The results obtained from computer modeling agrees quite well with the experimental result. Figure 7-9 for example, demonstrates a good correlation of the results obtained in the simulation procedure and experimental results. The relationship between the propagating modes depends on the refractive index of the fiber. It can be made strongly dependent on the temperature if an appropriate material and index profile is chosen. Consequently, optimizing the geometry of the fiber core/cladding structure, the glass composition, the core index profile and its temperature dependence – one can obtain an extremely high sensitivity IR sensing device.

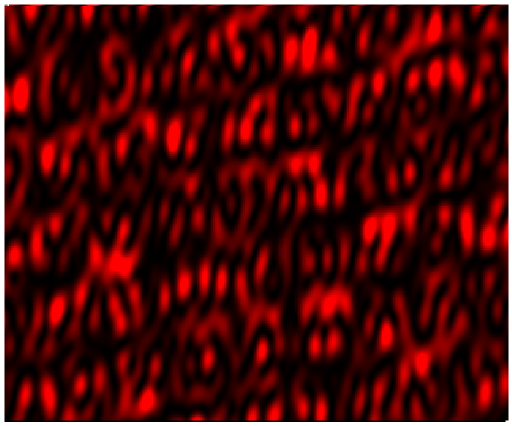

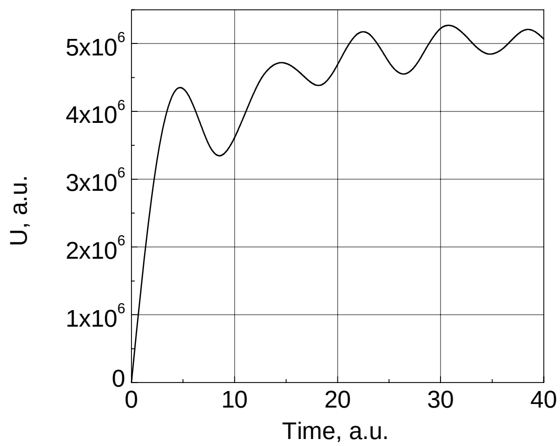

Fig. 7. Ilustration of the results of computer simulation: (a) computer simulation of the speckle image in the far-field of the fiber; (b) the output signal characteristic derived from computer simulation of the speckle image after switching on the IR radiation. The plot is for the ideal case of no noise. The number of modes m = 14.

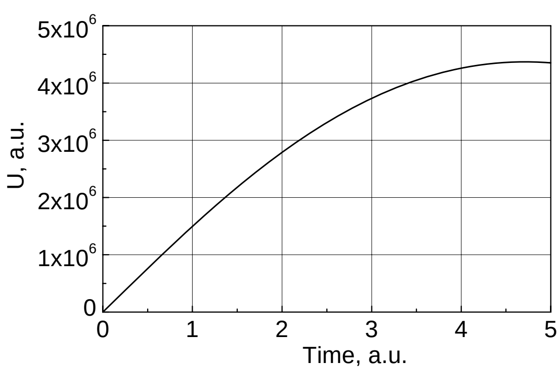

Fig. 8. Computer simulation of the output signal time dependence after switching on the IR radiation for the ideal case of no CCD noise. The number of modes was set at n = 14.

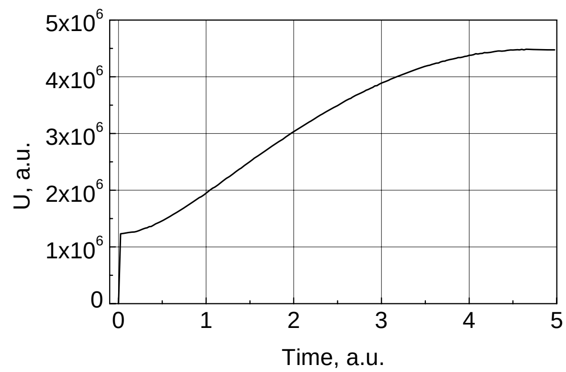

Fig. 9. Computer simulation of the output signal time dependence after switching on the IR radiation for the case of CCD noise. The number of modes was set at n = 14.

5. Summary

A high sensitivity fiber-optic method for registration of IR radiation has been proposed. The method is based on the effect of variation of the speckle pattern in the far-field of the fiber under the action of external perturbation. The IR radiation that falls on the multimode fiber leads to variation of the speckle image in the far field of the fiber. The variation of the phase difference between the propagating modes gives rise to variation of the speckle pattern in the far-filed of the fiber. Computer processing of the speckle image provides information on the amplitude of the perturbation that hits the fiber. The algorithm has been developed for processing of the speckle image and determining the amplitude of perturbation. Both experimental results as well as computer simulation data are presented. The method can be applied for measurement of temperature, IR radiation, vibrations amplitude, etc.

References

[1] J. W. Goodman, in Laser Speckle and Related Phenomena, J. C. Dainty, ed., Vol. 9 of Topics in Applied Physics, Springer-Verlag, New York, 1975.

[2] J. W. Goodman, Statistical Optics, Chap. 7, p. 350, Wiley, New York, 1985.

[3] D. Marcuse, Light Transmission Optics, New York, Van Nostrand Reinhold, 1972.

[4] 13.L.B. Soldano, E.C.M. Pennings, "Optical multi-mode interference devices based on self-imaging:principles and applications," IEEE J. Lightwave Technol. **13**, 615 (1995).

[5] R. Jones, C. Wykes, Holographic and speckle interferometry, Cambridge University Press, 1983.

[6] Jr. Spillman, Bb. William (Charlotte VT), "Multi mod optical fiber sensor and method", 08/31/1988, Int. Cl. G01B 9/02; US Cl. 356/345;250/227;356/354. Primary Cl. 356/477.

[7] Caputo Domenico and Palma Fabrizio, "System of infrared radiation detection based on sensors of amorpous silicon and its alloys", Pub. 1998-12-09; Index EP883194; Pat EP0883194; IPC H01L31/105; ECLA H01L31/105B.

[8] I. Culeac, „Optical devices based on optical fiber samples", In: "Contribution to Non-Crystalline Semiconductors and Optoelectronics", Ed. A.Buzdugan and M.Iovu, Chisinau 2003, p.26-39.

*Corresponding author: ion_culeac51@yahoo.com